

# Genome sequence of a 45,000-year-old modern human from western Siberia

Qiaomei Fu<sup>1,2</sup>, Heng Li<sup>3,4</sup>, Priya Moorjani<sup>3,5</sup>, Flora Jay<sup>6</sup>, Sergey M. Slepchenko<sup>7</sup>, Aleksei A. Bondarev<sup>8</sup>, Philip L. F. Johnson<sup>9</sup>, Ayinuer Aximu-Petri<sup>2</sup>, Kay Prüfer<sup>2</sup>, Cesare de Filippo<sup>2</sup>, Matthias Meyer<sup>2</sup>, Nicolas Zwyns<sup>10,11</sup>, Domingo C. Salazar-García<sup>10,12,13,14</sup>, Yaroslav V. Kuzmin<sup>15</sup>, Susan G. Keates<sup>15</sup>, Pavel A. Kosintsev<sup>16</sup>, Dmitry I. Razhev<sup>7</sup>, Michael P. Richards<sup>10,17</sup>, Nikolai V. Peristov<sup>18</sup>, Michael Lachmann<sup>2,19</sup>, Katerina Douka<sup>20</sup>, Thomas F. G. Higham<sup>20</sup>, Montgomery Slatkin<sup>6</sup>, Jean-Jacques Hublin<sup>10</sup>, David Reich<sup>3,4,21</sup>, Janet Kelso<sup>2</sup>, T. Bence Viola<sup>2,10</sup> & Svante Pääbo<sup>2</sup>

**We present the high-quality genome sequence of a ~45,000-year-old modern human male from Siberia. This individual derives from a population that lived before—or simultaneously with—the separation of the populations in western and eastern Eurasia and carries a similar amount of Neanderthal ancestry as present-day Eurasians. However, the genomic segments of Neanderthal ancestry are substantially longer than those observed in present-day individuals, indicating that Neanderthal gene flow into the ancestors of this individual occurred 7,000–13,000 years before he lived. We estimate an autosomal mutation rate of  $0.4 \times 10^{-9}$  to  $0.6 \times 10^{-9}$  per site per year, a Y chromosomal mutation rate of  $0.7 \times 10^{-9}$  to  $0.9 \times 10^{-9}$  per site per year based on the additional substitutions that have occurred in present-day non-Africans compared to this genome, and a mitochondrial mutation rate of  $1.8 \times 10^{-8}$  to  $3.2 \times 10^{-8}$  per site per year based on the age of the bone.**

In 2008, a relatively complete left human femoral diaphysis was discovered on the banks of the river Irtysh (Fig. 1a, c, d), near the settlement of Ust'-Ishim in western Siberia (Omsk Oblast, Russian Federation). Although the exact locality is unclear, the femur was eroding out of alluvial deposits on the left bank of the river, north of Ust'-Ishim. Here, Late Pleistocene and probably redeposited Middle Pleistocene fossils are found in sand and gravel layers that are about 50,000–30,000 years old (that is, from Marine Oxygen Isotope Stage 3).

## Morphology, dating and diet

The proximal end of the bone shows a large gluteal buttress and gluteal tuberosity, while the midshaft is dominated by a marked *linea aspera*, resulting in a teardrop-shaped cross-section (Fig. 1e, f) (for details, see Supplementary Information section 3). The morphology of the proximal end of the shaft is similar to Upper Paleolithic modern humans and distinct from Neanderthals (Supplementary Table 3.1, Supplementary Fig. 3.2.), while the teardrop-shaped cross section of the midshaft is similar to most Upper Paleolithic humans and early anatomically modern humans<sup>1</sup>. Taken together, this suggests that the Ust'-Ishim femur derives from a modern human.

Two samples of 890 mg and 450 mg of the bone were removed on separate occasions for dating. Collagen preservation satisfied all criteria for dating<sup>2</sup> and after ultrafiltration we obtained ages of  $41,400 \pm 1,300$  years before present (BP) (OxA-25516) and  $41,400 \pm 1,400$  BP (OxA-30190). These two dates, when combined and corrected for fluctuations of atmospheric <sup>14</sup>C through time, correspond to an age of about 45,000 calibrated

years BP (46,880–43,210 cal BP at 95.4% probability, Supplementary Information section 1). The Ust'-Ishim individual is therefore the oldest directly radiocarbon-dated modern human outside Africa and the Middle East (Fig. 1b). Carbon and nitrogen isotope ratios indicate that the diet of the Ust'-Ishim individual (Supplementary Information section 4) was based on terrestrial C<sub>3</sub> plants and animals that consumed them, but also that an important part of his dietary protein may have come from aquatic foods, probably freshwater fish, something that has been observed in other early Upper Palaeolithic humans from Europe<sup>3</sup>.

## DNA retrieval and sequencing

Nine samples of between 41 and 130 mg of bone material were removed from the distal part of the femur and used to construct DNA libraries using a protocol designed to facilitate the retrieval of short and damaged DNA<sup>4</sup>. The percentage of DNA fragments in these libraries that could be mapped to the human genome varied between 1.8% and 10.0% (Supplementary Table 1.1). From the extract containing the highest proportion of human DNA, eight further libraries were constructed. Each of these libraries was treated with uracil-DNA glycosylase and endonuclease VIII to remove deaminated cytosine residues, and library molecules with inserts shorter than approximately 35 base pairs (bp) were depleted by preparative acrylamide gel electrophoresis before sequencing on the Illumina HiSeq platform (Supplementary Information section 6). In total, 42-fold sequence coverage of the ~1.86 gigabases (Gb) of the autosomal genome to which short fragments can be confidently mapped was generated. The coverage of the X and Y chromosomes was approximately

<sup>1</sup>Key Laboratory of Vertebrate Evolution and Human Origins of Chinese Academy of Sciences, IVPP, CAS, Beijing 100044, China. <sup>2</sup>Department of Evolutionary Genetics, Max Planck Institute for Evolutionary Anthropology, D-04103 Leipzig, Germany. <sup>3</sup>Broad Institute of MIT and Harvard, Cambridge, Massachusetts 02142, USA. <sup>4</sup>Department of Genetics, Harvard Medical School, Boston, Massachusetts 02115, USA. <sup>5</sup>Department of Biological Sciences, Columbia University, New York, New York 10027, USA. <sup>6</sup>Department of Integrative Biology, University of California, Berkeley, California 94720-3140, USA. <sup>7</sup>Institute for Problems of the Development of the North, Siberian Branch of the Russian Academy of Sciences, Tyumen 625026, Russia. <sup>8</sup>Expert Criminalistics Center, Omsk Division of the Ministry of Internal Affairs, Omsk 644007, Russia. <sup>9</sup>Department of Biology, Emory University, Atlanta, Georgia 30322, USA. <sup>10</sup>Department of Human Evolution, Max Planck Institute for Evolutionary Anthropology, D-04103 Leipzig, Germany. <sup>11</sup>Department of Anthropology, University of California, Davis, California 95616, USA. <sup>12</sup>Department of Archaeology, University of Cape Town, Cape Town 7701, South Africa. <sup>13</sup>Departament de Prehistòria i Arqueologia, Universitat de València, Valencia 46010, Spain. <sup>14</sup>Research Group on Plant Foods in Hominin Dietary Ecology, Max-Planck Institute for Evolutionary Anthropology, D-04103 Leipzig, Germany. <sup>15</sup>Institute of Geology and Mineralogy, Siberian Branch of the Russian Academy of Sciences, Novosibirsk 630090, Russia. <sup>16</sup>Institute of Plant and Animal Ecology, Urals Branch of the Russian Academy of Sciences, Yekaterinburg 620144, Russia. <sup>17</sup>Laboratory of Archaeology, Department of Anthropology, University of British Columbia, Vancouver, British Columbia V6T 1Z1, Canada. <sup>18</sup>Siberian Cultural Center, Omsk 644010, Russia. <sup>19</sup>Santa Fe Institute, Santa Fe, New Mexico 87501, USA. <sup>20</sup>Oxford Radiocarbon Accelerator Unit, Research Laboratory for Archaeology and the History of Art, University of Oxford, Oxford OX1 3QY, UK. <sup>21</sup>Howard Hughes Medical Institute, Harvard Medical School, Boston, Massachusetts 02115, USA.

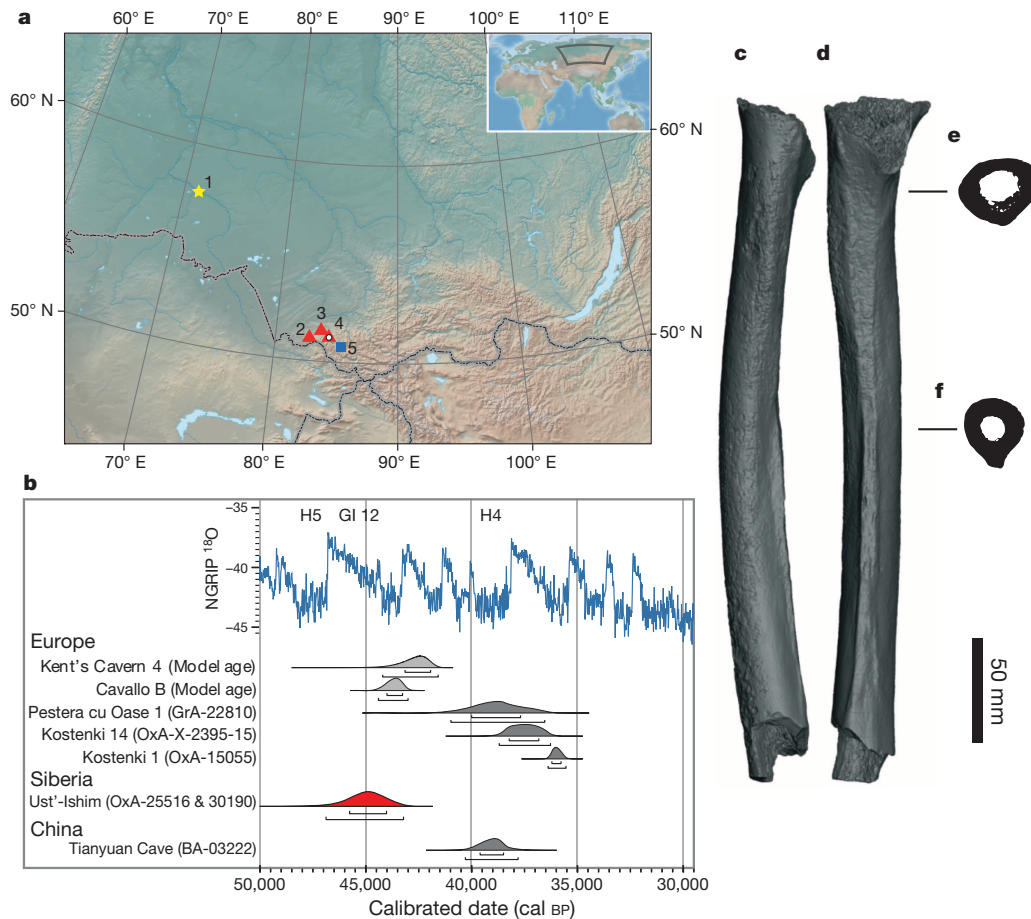


**Figure 1 | Geographic location, morphology and dating.** **a**, Map of Siberia with major archaeological sites. Red triangles: Neanderthal fossils; white circle within a red (Neanderthal) triangle: Denisovan fossils; blue square: Initial Upper Palaeolithic sites; yellow asterisk: Ust'-Ishim. 1: Ust'-Ishim; 2: Chagyrskaya Cave; 3: Okladnikov Cave; 4: Denisova Cave; 5: Kara-Bom. **b**, Radiocarbon ages of early modern human fossils in northern Eurasia and the NGRIP  $\delta^{18}\text{O}$  palaeotemperature record. Specimens in light grey are indirectly

dated (OxCal v4.2.3 (ref. 33); r:5 IntCal13 atmospheric curve<sup>34</sup>). H5: Heinrich 5 event, H4: Heinrich 4 event, GI 12: Greenland Interstadial 12. For a more extensive comparison see Supplementary Information Fig. 2.1. **c-f**, The Ust'-Ishim 1 femur. **c**, Lateral view. **d**, Posterior view. **e**, Cross-section at the 80 percent level. **f**, Cross-section at the midshaft. For other views see Supplementary Fig. 3.1.

half that of the autosomes ( $\sim 22$ -fold), indicating that the bone comes from a male. A likelihood method estimated present-day human mitochondrial DNA (mtDNA) contamination<sup>5</sup> to 0.50% (95% confidence interval (CI) 0.26–0.94%), whereas a method that uses the frequency of non-consensus bases in autosomal sequences estimated the contamination to be less than 0.13% (Supplementary Information section 7). Thus, less than 1% of the hominin DNA fragments sequenced are estimated to be extraneous to the bone. After consensus genotype calling, such low levels of contamination will tend to be eliminated.

### Population relationships

About 7.7 positions per 10,000 are heterozygous in the Ust'-Ishim genome, whereas between 9.6 and 10.5 positions are heterozygous in present-day Africans and 5.5 and 7.7 in present-day non-Africans (Supplementary Information section 12). Thus, with respect to genetic diversity, the population to which the Ust'-Ishim individual belonged was more similar to present-day Eurasians than to present-day Africans, which probably reflects the out-of-Africa bottleneck shared by non-African populations. The Ust'-Ishim mtDNA sequence falls at the root of a large group of related mtDNAs (the 'R haplogroup'), which occurs today across Eurasia (Supplementary Information section 8). The Y chromosome sequence of the Ust'-Ishim individual is similarly inferred to be ancestral to a group of related Y chromosomes (haplogroup K(xLT)) that occurs across Eurasia today<sup>6</sup> (Supplementary Information section 9). As expected, the number of mutations inferred to have occurred on the

branch leading to the Ust'-Ishim mtDNA is lower than the numbers inferred to have occurred on the branches leading to related present-day mtDNAs (Supplementary Fig. 8.1). Using this observation and nine directly carbon-dated ancient modern human mtDNAs as calibration points<sup>5,7</sup> in a relaxed molecular clock model, we estimate the age of the Ust'-Ishim bone to be  $\sim 49,000$  years BP (95% highest posterior density: 31,000–66,000 years BP), consistent with the radiocarbon date.

In a principal component analysis of the Ust'-Ishim autosomal genome along with genotyping data from 922 present-day individuals from 53 populations<sup>8</sup> (Fig. 2a), the Ust'-Ishim individual clusters with non-Africans rather than Africans. When only non-African populations are analysed (Fig. 2b), the Ust'-Ishim individual falls close to zero on the two first principal component axes, suggesting that it does not share much more ancestry with any particular group of present-day humans. To determine how the Ust'-Ishim genome is related to the genomes of present-day humans, we tested, using  $D$  statistics<sup>8</sup>, whether it shares more derived alleles with one modern human than with another modern human using pairs of human genomes from different parts of the world (Fig. 3). Based on genotyping data for 87 African and 108 non-African individuals (Supplementary Information section 11), the Ust'-Ishim genome shares more alleles with non-Africans than with sub-Saharan Africans ( $|Z| = 41\text{--}89$ ), consistent with the principal component analysis, mtDNA and Y chromosome results. Thus, the Ust'-Ishim individual represents a population derived from, or related to, the population involved in the dispersal of modern humans out of Africa. Among the non-Africans,

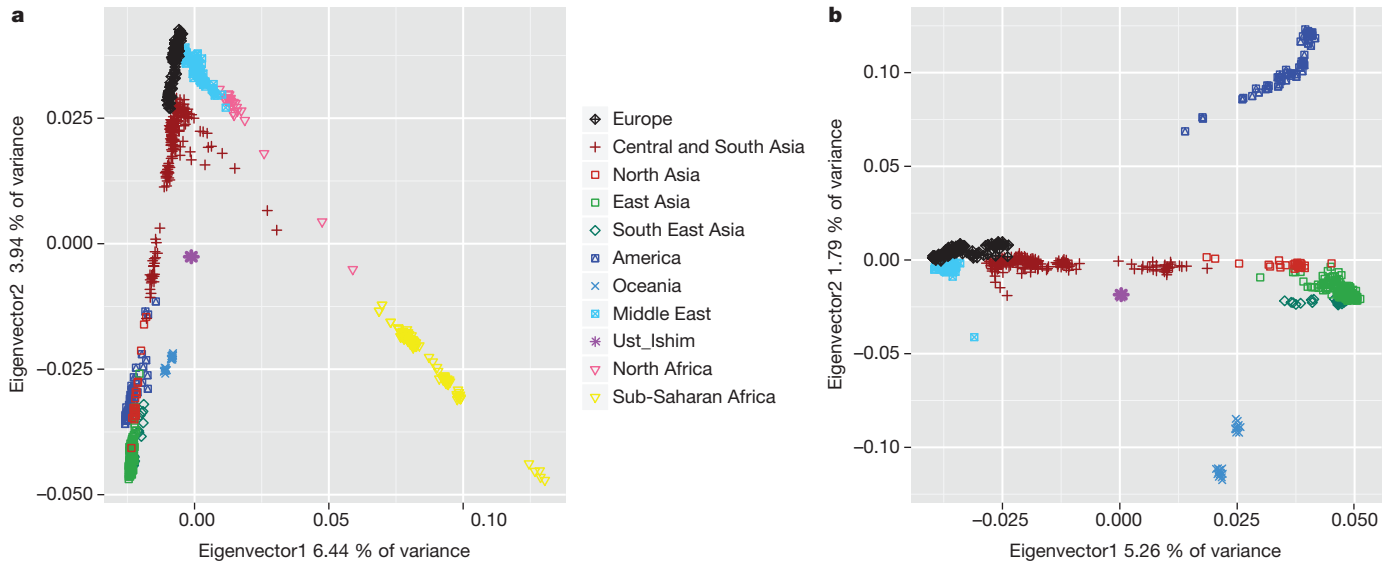


**Figure 2 | Principal Components (PC) analysis exploring the relationship of Ust'-Ishim to present-day humans.** **a**, PC analysis using 922 present-day individuals from 53 populations and the Ust'-Ishim individual. **b**, PC analysis

using Eurasian individuals and the Ust'-Ishim individual. The percentages of the total variance explained by each eigenvector are given.

the Ust'-Ishim genome shares more derived alleles with present-day people from East Asia than with present-day Europeans ( $|Z| = 2.1-6.4$ ). However, when an ~8,000-year-old genome from western Europe (La Braña)<sup>9</sup> or a 24,000-year-old genome from Siberia (Mal'ta 1)<sup>10</sup> were analysed, there is no evidence that the Ust'-Ishim genome shares more derived alleles with present-day East Asians than with these prehistoric individuals ( $|Z| < 2$ ). This suggests that the population to which the Ust'-Ishim individual belonged diverged from the ancestors of present-day

West Eurasian and East Eurasian populations before—or simultaneously with—their divergence from each other. The finding that the Ust'-Ishim individual is equally closely related to present-day Asians and to 8,000- to 24,000-year-old individuals from western Eurasia, but not to present-day Europeans, is compatible with the hypothesis that present-day Europeans derive some of their ancestry from a population that did not participate in the initial dispersals of modern humans into Europe and Asia<sup>11</sup>.

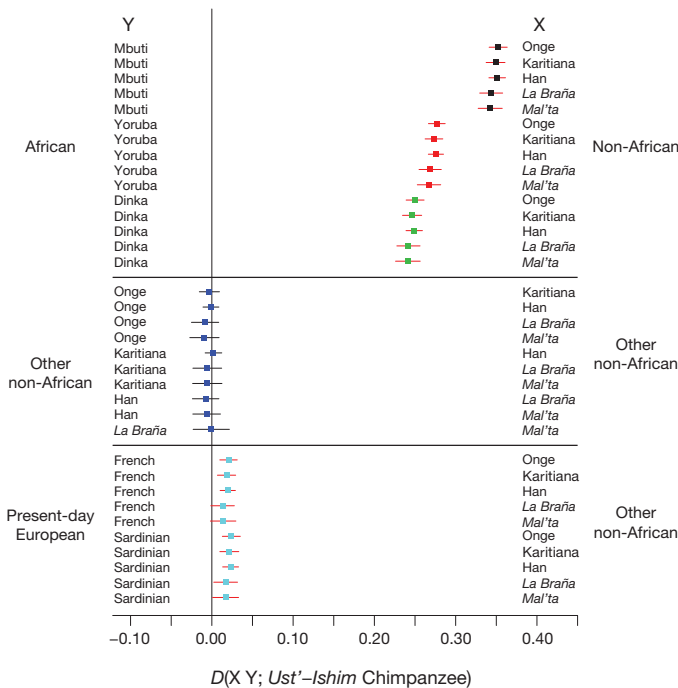


**Figure 3 | Statistics testing whether the Ust'-Ishim genome shares more derived alleles with one or the other of two modern human genomes (X, Y).** We computed  $D$  statistics of the form  $D(X, Y, \text{Ust}'\text{-Ishim, Chimpanzee})$  using a subset of the genome-wide SNP array data from the Affymetrix Human Origins array and restricting the analysis to transversions. Error bars correspond to three standard errors. Red bars indicate that the  $D$  statistic is significantly different from 0 ( $|Z| > 2$ ), such that the Ust'-Ishim genome shares more derived alleles with the genome on the right (X) than the left (Y). Ancient genomes are given in italics.

### Mutation rate estimates

The high-quality Ust'-Ishim genome sequence, in combination with its radiocarbon date, allows us to gauge the rate of mutations by estimating the numbers of mutations that are 'missing' in the Ust'-Ishim individual relative to present-day humans. This results in a mutation rate estimate of  $0.44 \times 10^{-9}$  to  $0.63 \times 10^{-9}$  per site per year using the high-coverage genomes of 14 present-day humans. A challenge for inferring the mutation rate in this way is that differences in error rates among genome sequences can confound the inference (see discussion in ref. 12). We therefore developed an alternative approach that leverages the Pairwise Sequentially Markovian Coalescent (PSMC), a method which estimates the distribution of coalescence times between the two chromosomes across a diploid genome to estimate past changes in population size<sup>13</sup>, and which is less influenced by differences in error rates. When the Ust'-Ishim genome along with 25 present-day human genomes are analysed by PSMC, a recent reduction in population size similar to that seen for 11 present-day non-Africans is inferred for the Ust'-Ishim genome. However, the apparent age of this size reduction is more recent than in present-day humans, consistent with the Ust'-Ishim genome being older (Fig. 4). We then compute the number of additional substitutions that are needed to best fit the Ust'-Ishim PSMC curve to those of other non-African genomes. Assuming that this corresponds to the number of mutations that have accumulated over around 45,000 years, we estimate a mutation rate of  $0.43 \times 10^{-9}$  per site per year (95% CI  $0.38 \times 10^{-9}$  to  $0.49 \times 10^{-9}$ ) that is consistent across all non-African genomes regardless of their coverage (Supplementary Information section 14). This overall rate, as well as the relative rates inferred for different mutational classes (transversions, non-CpG transitions, and CpG transitions), is similar to the rate observed for *de novo* estimates from human pedigrees ( $\sim 0.5 \times 10^{-9}$  per site per year<sup>14,15</sup>) and to the direct estimate of branch shortening (Supplementary Information section 10). As discussed elsewhere<sup>14,16,17</sup>, these rates are slower than those estimated using calibrations based on the fossil record and thus suggest older dates for the splits of modern

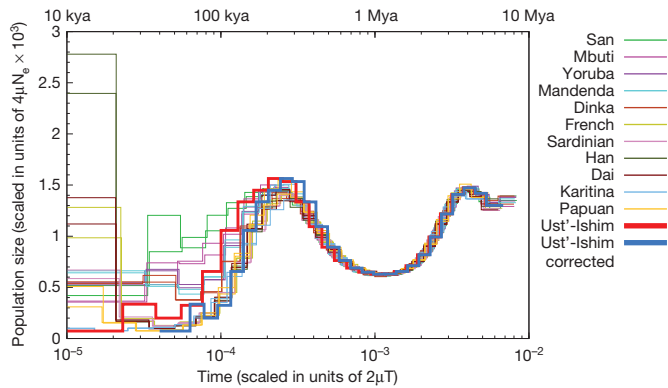


**Figure 4 | Inferred population size changes over time.** ‘Time’ on the *x* axis refers to the pairwise per-site sequence divergence. If we erroneously assume that Ust'-Ishim lived today, its inferred population size history includes an out-of-Africa-like population bottleneck that is more recent than that seen in present-day non-Africans (red bold curve). By shifting the Ust'-Ishim curve to align with those in present-day non-Africans (blue bold curve), and assuming that the number of mutations necessary to do this corresponds to 45,000 years, we estimate the autosomal mutation rate to be  $0.38 \times 10^{-9}$  to  $0.49 \times 10^{-9}$  per site per year. The times indicated on the top of the figure are based on this mutation rate.

human and archaic populations. We caution, however, that rates may have changed over time and may differ between human populations. However, we expect this mutation rate estimate to apply at least to non-African populations over the past 45,000 years.

We also estimated a phylogeny relating the non-recombining part of the Ust'-Ishim Y chromosome to those of 23 present-day males. Using this phylogeny, we measured the number of ‘missing’ mutations in the Ust'-Ishim Y chromosomal lineage relative to the most closely related present-day Y chromosome analysed. This results in an estimate of the Y chromosome mutation rate of  $0.76 \times 10^{-9}$  per site per year (95% CI  $0.67 \times 10^{-9}$  to  $0.86 \times 10^{-9}$ ) (Supplementary Information section 9), significantly higher than the autosomal mutation rate, consistent with mutation rates in males being higher than in females<sup>18–20</sup>. Finally, using the radiocarbon date of the Ust'-Ishim femur together with the mtDNAs of 311 present-day humans, we estimated the mutation rate of the complete mtDNA to be  $2.53 \times 10^{-8}$  substitutions per site per year (95% highest posterior density:  $1.76 \times 10^{-8}$  to  $3.23 \times 10^{-8}$ ) (Supplementary Information section 8) for mtDNA, in agreement with a previous study<sup>5</sup>.

## Neanderthal admixture

The time of admixture between modern humans and Neanderthals has previously been estimated to 37,000–86,000 years BP based on the size

of the DNA segments contributed by Neanderthals to present-day non-Africans<sup>21</sup>. Thus, the Ust'-Ishim individual could pre-date the Neanderthal admixture. From the extent of sharing of derived alleles between the Neanderthal and the Ust'-Ishim genomes we estimate the proportion of Neanderthal admixture in the Ust'-Ishim individual to be  $2.3 \pm 0.3\%$  (Supplementary Information section 16), similar to present-day east Asians (1.7–2.1%) and present-day Europeans (1.6–1.8%). Thus, admixture with Neanderthals had already occurred by 45,000 years ago. In contrast, we fail to detect any contribution from Denisovans, although such a contribution exists in present-day people not only in Oceania<sup>22,23</sup>, but to a lesser extent also in mainland east Asia<sup>12,24</sup> (Supplementary Information section 17).

The DNA segments contributed by Neanderthals to the Ust'-Ishim individual are expected to be longer than such segments in present-day people as the Ust'-Ishim individual lived closer in time to when the admixture occurred, so there was less time for the segments to be fragmented by recombination. To test if this is indeed the case, we identified putative Neanderthal DNA segments in the Ust'-Ishim and present-day genomes based on derived alleles shared with the Neanderthal genome at positions where Africans are fixed for ancestral alleles. Figure 5 shows that fragments of putative Neanderthal origin in the Ust'-Ishim individual are substantially longer than those in present-day humans. We use the covariance in such derived alleles of putative Neanderthal origin across the Ust'-Ishim genome to infer that mean fragment sizes in the Ust'-Ishim genome are in the order of  $\sim 1.8$ – $4.2$  times longer than in present-day genomes and that the Neanderthal gene flow occurred 232–430 generations before the Ust'-Ishim individual lived (Supplementary Information section 18; Fig. 6). Under the simplifying assumption that the gene flow occurred as a single event, and assuming a generation time of 29 years<sup>16,25</sup>, we estimate that the admixture between the ancestors of the Ust'-Ishim individual and Neanderthals occurred approximately 50,000 to 60,000 years BP, which is close to the time of the major expansion of modern humans out of Africa and the Middle East. However, we also note that the presence of some longer fragments (Fig. 5) may indicate that additional admixture occurred even later. Nevertheless, these results suggest that the bulk of the Neanderthal contribution to present-day people outside Africa does not go back to mixture between Neanderthals and the anatomically modern humans who lived in the Middle East at earlier times; for example, the modern humans whose remains have been found at Skhul and Qafzeh<sup>26,27</sup>.

## An Initial Upper Paleolithic individual?

A common model for the modern human colonization of Asia<sup>23,28</sup> assumes that an early coastal migration gave rise to the present-day people of Oceania, while a later more northern migration gave rise to Europeans and mainland Asians. The fact that the 45,000-year-old individual from Siberia is not more closely related to the Onge from the Andaman

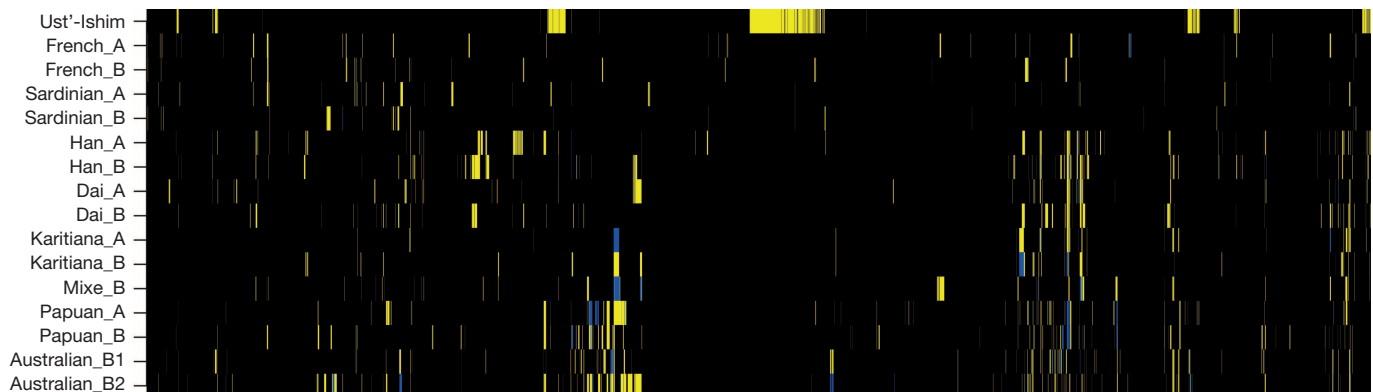


**Figure 5 | Regions of Neanderthal ancestry on chromosome 12 in the Ust'-Ishim individual and fifteen present-day non-Africans.** The analysis is based on SNPs where African genomes carry the ancestral allele and the

Neanderthal genome carries the derived allele. Homozygous ancestral alleles are black, heterozygous derived alleles yellow, and homozygous derived alleles blue.

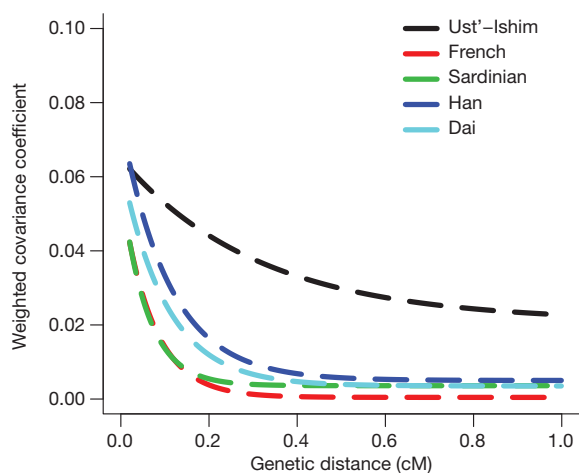


**Figure 6 | Dating the Neanderthal admixture in Ust'-Ishim and present-day non-Africans.** Exponentially fitted curves showing the decay of pairwise covariance for variable positions where Africans carry ancestral alleles and the Neanderthal genome carries derived alleles.

Islands (putative descendants of an early coastal migration) than he is to present-day East Asians or Native Americans (putative descendants of a northern migration) (Fig. 3) shows that at least one other group to which the ancestors of the Ust'-Ishim individual belonged colonized Asia before 45,000 years ago. Interestingly, the Ust'-Ishim individual probably lived during a warm period (Greenland Interstadial 12) that has been proposed to be a time of expansion of modern humans into Europe<sup>29,30</sup>. However, the latter hypothesis is based only on the appearance of the so-called 'Initial Upper Paleolithic' industries (Supplementary Information section 5), and not on the identification of modern human remains<sup>31,32</sup>. It is possible that the Ust'-Ishim individual was associated with the Asian variant of Initial Upper Paleolithic industry, documented at sites such as Kara-Bom in the Altai Mountains at about 47,000 years BP. This individual would then represent an early modern human radiation into Europe and Central Asia that may have failed to leave descendants among present-day populations<sup>29</sup>.

**Online Content** Methods, along with any additional Extended Data display items and Source Data, are available in the online version of the paper; references unique to these sections appear only in the online paper.

**Received 15 May; accepted 29 August 2014.**

1. Trinkaus, E. & Ruff, C. B. Diaphyseal cross-sectional geometry of Near Eastern Middle Paleolithic humans: the femur. *J. Archaeol. Sci.* **26**, 409–424 (1999).
2. Brock, F. *et al.* Reliability of nitrogen content (%N) and carbon:nitrogen atomic ratios (C:N) as indicators of collagen preservation suitable for radiocarbon dating. *Radiocarbon* **54**, 879–886 (2012).
3. Richards, M. P. & Trinkaus, E. Out of Africa: modern human origins special feature: isotopic evidence for the diets of European Neanderthals and early modern humans. *Proc. Natl Acad. Sci. USA* **106**, 16034–16039 (2009).
4. Meyer, M. *et al.* A high-coverage genome sequence from an archaic Denisovan individual. *Science* **338**, 222–226 (2012).
5. Fu, Q. *et al.* A revised timescale for human evolution based on ancient mitochondrial genomes. *Curr. Biol.* **23**, 553–559 (2013).
6. The Y Chromosome Consortium A nomenclature system for the tree of human Y-chromosomal binary haplogroups. *Genome Res.* **12**, 339–348 (2002).
7. Shapiro, B. *et al.* A Bayesian phylogenetic method to estimate unknown sequence ages. *Mol. Biol. Evol.* **28**, 879–887 (2011).
8. Patterson, N. *et al.* Ancient admixture in human history. *Genetics* **192**, 1065–1093 (2012).
9. Olalde, I. *et al.* Derived immune and ancestral pigmentation alleles in a 7,000-year-old Mesolithic European. *Nature* **507**, 225–228 (2014).
10. Raghavan, M. *et al.* Upper Palaeolithic Siberian genome reveals dual ancestry of Native Americans. *Nature* **505**, 87–91 (2014).
11. Lazaridis, I. *et al.* Ancient human genomes suggest three ancestral populations for present-day Europeans. *Nature* **513**, 409–413 (2014).
12. Prüfer, K. *et al.* The complete genome sequence of a Neanderthal from the Altai Mountains. *Nature* **505**, 43–49 (2014).

13. Li, H. & Durbin, R. Inference of human population history from individual whole-genome sequences. *Nature* **475**, 493–496 (2011).
14. Scally, A. & Durbin, R. Revising the human mutation rate: implications for understanding human evolution. *Nature Rev. Genet.* **13**, 745–753 (2012).
15. Kong, A. *et al.* Rate of *de novo* mutations and the importance of father's age to disease risk. *Nature* **488**, 471–475 (2012).
16. Langergraber, K. E. *et al.* Generation times in wild chimpanzees and gorillas suggest earlier divergence times in great ape and human evolution. *Proc. Natl Acad. Sci. USA* **109**, 15716–15721 (2012).
17. Prüfer, K. *et al.* The bonobo genome compared with the chimpanzee and human genomes. *Nature* **486**, 527–531 (2012).
18. Xue, Y. *et al.* Human Y chromosome base-substitution mutation rate measured by direct sequencing in a deep-rooting pedigree. *Curr. Biol.* **19**, 1453–1457 (2009).
19. Kuroki, Y. *et al.* Comparative analysis of chimpanzee and human Y chromosomes unveils complex evolutionary pathway. *Nature Genet.* **38**, 158–167 (2006).
20. Wang, J., Fan, H. C., Behr, B. & Quake, S. R. Genome-wide single-cell analysis of recombination activity and *de novo* mutation rates in human sperm. *Cell* **150**, 402–412 (2012).
21. Sankararaman, S., Patterson, N., Li, H., Pääbo, S. & Reich, D. The date of interbreeding between Neanderthals and modern humans. *PLoS Genet.* **8**, e1002947 (2012).
22. Reich, D. *et al.* Genetic history of an archaic hominin group from Denisova Cave in Siberia. *Nature* **468**, 1053–1060 (2010).
23. Reich, D. *et al.* Denisova admixture and the first modern human dispersals into Southeast Asia and Oceania. *Am. J. Hum. Genet.* **89**, 516–528 (2011).
24. Skoglund, P. & Jakobsson, M. Archaic human ancestry in East Asia. *Proc. Natl Acad. Sci. USA* **108**, 18301–18306 (2011).
25. Fenner, J. N. Cross-cultural estimation of the human generation interval for use in genetics-based population divergence studies. *Am. J. Phys. Anthropol.* **128**, 415–423 (2005).
26. McCown, T. D. & Keith, A. *The Stone Age of Mount Carmel* Vol. 2 (Clarendon, Oxford, 1939).
27. Vandermeersch, B. *Les Hommes Fossiles de Qafzeh (Israel)* 319 (Éditions du CNRS, 1981).
28. Rasmussen, M. *et al.* An Aboriginal Australian genome reveals separate human dispersals into Asia. *Science* **334**, 94–98 (2011).
29. Hublin, J. J. The earliest modern human colonization of Europe. *Proc. Natl Acad. Sci. USA* **109**, 13471–13472 (2012).
30. Müller, U. C. *et al.* The role of climate in the spread of modern humans into Europe. *Quat. Sci. Rev.* **30**, 273–279 (2011).
31. Goebel, T. A., Derevianko, A. P. & Petrin, V. T. Dating the Middle to Upper Paleolithic transition at Kara-Bom. *Curr. Anthropol.* **34**, 452–458 (1993).
32. Kuhn, S. L. & Zwyns, N. Rethinking the initial Upper Paleolithic. *Quat. Int.* <http://dx.doi.org/10.1016/j.quaint.2014.05.040> (2014).
33. Bronk Ramsey, C., Scott, M. & van der Plicht, H. Calibration for archaeological and environmental terrestrial samples in the time range 26–50 ka cal BP. *Radiocarbon* **55**, 2021–2027 (2013).
34. Reimer, P. J. *et al.* IntCal13 and Marine13 radiocarbon age calibration curves 0–50,000 Years cal BP. *Radiocarbon* **55**, 1869–1887 (2009).

**Supplementary Information** is available in the online version of the paper.

**Acknowledgements** We are grateful to P. Gunz, M. Kircher, A. I. Krivoschapkin, P. Nigst, M. Ongyerth, N. Patterson, G. Renaud, U. Stenzel, M. Stoneking and S. Talamo for valuable input, comments and help; T. Pfisterer and H. Temming for technical assistance. Q.F. is funded in part by the Chinese Academy of Sciences (XDA05130202) and the Ministry of Science and Technology of China (2007FY110200); P.A.K. by Urals Branch, Russian Academy of Sciences (12-C-4-1014) and Y.V.K. by the Russian Foundation for Basic Sciences (12-06-00045); F.J. and M.S. by the National Institutes of Health of the USA (R01-GM40282); P.J. by the NIH (K99-GM104158); and T.F.G.H. by ERC advanced grant 324139. D.R. is a Howard Hughes Medical Institute Investigator and supported by the National Science Foundation (1032255) and the NIH (GM100233). Major funding for this work was provided by the Presidential Innovation Fund of the Max Planck Society.

**Author Contributions** Q.F., S.M.S., A.A.B., Y.V.K., J.K., T.B.V. and S.P. designed the research. A.A.P. and Q.F. performed the experiments; Q.F., H.L., P.M., F.J., P.L.F.J., K.P., C.d.F., M.M., M.L., M.S., D.R., J.K. and S.P. analysed genetic data; K.D. and T.F.G.H. performed <sup>14</sup>C dating; D.C.S.-G. and M.P.R. analysed stable isotope data; N.V.P., P.A.K. and D.I.R. contributed samples and data; S.M.S., A.A.B., N.Z., Y.V.K., S.G.K., J.-J.H. and T.B.V. analysed archaeological and anthropological data; Q.F., J.K., T.B.V. and S.P. wrote and edited the manuscript with input from all authors.

**Author Information** All sequence data have been submitted to the European Nucleotide Archive (ENA) and are available under the following Ust'-Ishim accession number: PRJEB6622. The data from the 25 present-day human genomes are available from (<http://www.simonsfoundation.org/life-sciences/simons-genome-diversity-project/>) and from (<http://cdna.eva.mpg.de/neandertal/altai/>). Reprints and permissions information is available at [www.nature.com/reprints](http://www.nature.com/reprints). The authors declare no competing financial interests. Readers are welcome to comment on the online version of the paper. Correspondence and requests for materials should be addressed to Q.F. (qiamei\_fu@eva.mpg.de), D.R. (reich@genetics.med.harvard.edu), J.K. (kelso@eva.mpg.de) or T.B.V. (bence\_viola@eva.mpg.de).

## METHODS

All sequencing was performed on the Illumina HiSeq 2000 and base-calling was carried out using Ibis 1.1.6.9 (ref. 35). Reads were merged and remaining adaptor sequences trimmed before being aligned to the Human reference genome (GRCh37/1000 Genomes) using BWA (version 0.5.10)<sup>36</sup>. GATK version 1.3 (v1.3-14-g348f2b) was used to produce genotype calls for each site. We excluded from analysis tandem repeats and regions of the genome that are not unique. We considered only

genomic regions that fall within the 95% coverage distribution (Supplementary Information section 7) and where at least 99% of overlapping 35mers covering a position map uniquely, allowing one mismatch.

35. Kircher, M., Stenzel, U. & Kelso, J. Improved base calling for the Illumina Genome Analyzer using machine learning strategies. *Genome Biol.* **10**, R83 (2009).
36. Li, H. & Durbin, R. Fast and accurate short read alignment with Burrows–Wheeler transform. *Bioinformatics* **25**, 1754–1760 (2009).